SUPPORTING INFORMATION

For

Fibrillar and non-fibrillar amyloid beta structures drive two modes of membrane-mediated toxicity

Crystal M. Vander Zanden[1-3], Lois Wampler[4], Isabella Bowers[5], Erik B. Watkins[6], Jaroslaw Majewski[2,7,8] and Eva Y. Chi[1,2*]

[1]Center for Biomedical Engineering, University of New Mexico, Albuquerque, NM 87131. [2]Department of Chemical and Biological Engineering, University of New Mexico, Albuquerque, NM 87131. [3]Department of Chemistry and Biochemistry, University of Colorado Colorado Springs, Colorado Springs, CO 80918. [4]Department of Biomedical Engineering, Texas A&M University, College Station, TX 77843. [5]Department of Engineering and Technology, Southeast Missouri State University, Cape Girardeau, MO 63701. [6]MPA-11: Materials Synthesis and Integrated Devices, Los Alamos National Laboratory, Los Alamos, NM 87545. [7]Division of Molecular and Cellular Biosciences, National Science Foundation, Alexandria, VA 22314. [8]Theoretical Biology and Biophysics, Los Alamos National Laboratory, Los Alamos, New Mexico 87545.

*Present address: 210 University Blvd. NE, University of New Mexico. Albuquerque, NM 87131

*To whom correspondence should be addressed: Eva Y. Chi: Department of Chemical and Biological Engineering, University of New Mexico, Albuquerque, NM, USA; evachi@unm.edu; Tel. (505) 277-2263

Supplemental Experimental Procedures

X-ray scattering data analysis:

X-ray reflectivity (XR) measurements were made to determine the electron density distribution of materials (lipids and proteins) at the air/water interface on a Langmuir trough along the surface normal. X-ray scattering theory and liquid diffractometer methods have been previously described[39–41] and the intensity of reflected X-rays can be used to deduce detailed information on the electron density distribution normal to the interface, $\rho(z)$. To change the angle of incidence on the sample, a Germanium monochromator crystal was tilted to deflect the beam and to reach the range of vertical momentum transfer vector values $0.01 < q_z < 0.8$ Å^{-1}. Reflected intensities were background subtracted and normalized to incident beam flux. For better visualization, the X-ray reflectivities were normalized to the Fresnel reflectivity (scattering from an infinitely sharp air-water interface) with error bars representing one standard deviation of the measurement. A 'slab' model of molecular layers with distinct electron densities was used to fit reflectivity data to obtain the $\rho(z)$[24]. The studied system was divided into layers, each of certain thickness and ρ, and interconnected by interfacial roughnesses approximated by error functions. The Motofit program[42] implemented within the scientific data analysis software IGOR Pro was used for parameter fitting, and goodness of fit was monitored by χ^2 values.

For GIXD experiments, an incident beam striking the water surface at a momentum transfer vector $q_z = 0.85 \cdot q_c$, where $q_c = 0.02176$ Å^{-1} is the critical scattering vector for total external reflection from the subphase. At this q_z, an evanescent wave is generated which travels along the surface and can Bragg scatter from the molecular arrangements at the interface. The scattered intensity was measured by a 2-D detector over a range of horizontal and vertical scattering vectors q_{xy} and q_z: $q_{xy} \sim (4\pi/\lambda)\sin(2\theta_{xy}/2)$, where $2\theta_{xy}$ is the angle between the incident and diffracted beam projected on the liquid surface and $q_z=(2\pi/\lambda)\sin\alpha$, where α is the vertical scattering angle. Bragg peaks resolved in the q_{xy} but integrated over the q_z direction represent GIXD intensity resulting from a powder of 2-D crystallites. After background subtraction of the GIXD data, the Bragg peaks were fit with the Multi Peak Fit 2 function for IGOR Pro using Gaussian, Lorentzian, or Voigt profiles to optimize the goodness of fit. For Voigt profile fits, a conservative 15% error is assumed for the full width half maximum (FWHM) values. The *d*-

spacings are determined by the angular positions of the Bragg peaks, $d = 2\pi/q_{xy}^{max}$ (where q_{xy}^{max} is the center of the Bragg peak) for the 2-D lattice. Areas under peaks were also obtained.

The coherence length (L_c) of the 2-D crystallites is calculated from the resolution-corrected FWHM of the peaks using the Scherrer formula[43]. The q_{xy} resolution of the ChemMatCARS liquid surface instrument, Δq_{xy} = 0.006 Å^{-1}, was taken into consideration to calculate the intrinsic FWHM values. The average distance in the direction of the reciprocal lattice vector q_{xy} over which ordering extends, can be determined using Equation 1.

$$L_c = \frac{0.9 \times 2\pi}{\sqrt{FWHM^2 - 0.006^2}} \quad (1)$$

Supplementary Figures and Tables:

Table S1: XR fit parameters for Aβ_m, FO, and NFO adsorbed to an air/water interface

	Slab 1 (Protein)			Subphase	
	Thickness	ρ / ρ_{water}	Roughness	Roughness	χ^2
Aβ_m	18.85 ± 0.18	1.285 ± 0.003	2.882 ± 0.006	10.04± 0.18	5.6
FO	18.90 ± 0.19	1.316 ± 0.003	2.827 ± 0.006	10.49 ± 0.19	6.0
NFO	15.90 ± 0.14	1.314 ± 0.003	2.730 ± 0.007	7.96 ± 0.13	4.1

Table S2: Calculated values from GIXD fitting parameters obtained from protein diffraction peaks of Aβ adsorbed to an air/water interface.

Sample	***q_{xy}* Position (Å^{-1})**	***FWHM****	***d Spacing* (Å)**	***Integrated Peak Area***	***Coherence Length* L_c (Å)***
		β-*Sheet Diffraction Peaks*			
Aβ_m	1.329 ± 0.008	0.064 ± 0.010	4.727 ± 0.03	100 ± 30	87 ± 13
FO	1.326 ± 0.008	0.074 ± 0.011	4.739 ± 0.03	180 ± 50	76 ± 11
NFO	1.328 ± 0.009	0.070 ± 0.011	4.731 ± 0.03	150 ± 50	80 ± 12
		Higher Order Diffraction Peaks			
Aβ_m	0.152 ± 0.007	0.032 ± 0.005	41.2 ± 1.8	120 ± 60	180 ± 30

*A conservative 15% error was assumed

Table S3: XR fit parameters for DMPG monolayer alone and after addition of Aβ_m, FO, or NFO

	Slab 1 (Tails)			Slab 2 (Heads)			Slab 3 (outside layer)			Subphase	
	Thickness	ρ / ρ_{water}	Roughness	Thickness	ρ / ρ_{water}	Roughness	Thickness	ρ / ρ_{water}	Roughness	Roughness	χ^2
DMPG	15.9 ± 0.2	0.97 ± 0.03	3.27 ± 0.3	9.1 ± 0.3	1.58 ± 0.02	3.4 ± 0.2	/	/	/	2.8 ± 0.4	7.84
DMPG + Aβ_m	14.67 ± 0.03	1.057 ± 0.004	4.41 ± 0.02	9.4 ± 0.4	1.534 ± 0.007	3.7	34.0 ± 0.3	1.154 ± 0.002	11.1	8.59 ± 0.17	0.83
DMPG + FO	13.21 ± 0.04	0.940 ± 0.004	4.0	9.1 ± 0.4	1.552 ± 0.013	5.1	37.4 ± 0.6	1.171 ± 0.004	11.6 ± 0.4	10.5 ± 0.3	1.83
DMPG + NFO	16.0± 0.2	0.98 ± 0.03	3.32 ± 0.04	9.3 ± 0.3	1.53 ± 0.03	3.4 ± 0.2	/	/	/	2.93 ± 0.10	5.2

Table S4: Calculated values from GIXD fitting parameters obtained from lipid and protein diffraction peaks of Aβ binding to a DMPG monolayer.

Sample	***q_{xy} Position ($Å^{-1}$)***	***FWHM***	***d Spacing (Å)***	***Inter-Molecule Distance (Å)*****	***Integrated Peak Area***	***Coherence Length L_c (Å)***	***Surface Pressure (mN/m)***
Protein + DMPG: Lipid Diffraction Peaks							
DMPG	1.491 ± 0.006	0.0133 ± 0.0003	4.214 ± 0.017	4.87 ± 0.02	704 ± 12	469 ± 12	25.0
DMPG + Aβ_m	1.485 ± 0.006	0.0274 ± 0.0012	4.232 ± 0.018	4.89 ± 0.02	369 ±10	209 ± 9	35.8
DMPG + FO	1.489 ± 0.007	0.0218 ± 0.0012	4.220 ± 0.018	4.87 ± 0.02	229 ± 9	269 ± 14	37.0
DMPG + NFO	1.490 ± 0.007	0.0172 ± 0.0017	4.216 ± 0.019	4.87 ± 0.02	138 ± 10	350 ± 30	30.0
Protein + DMPG: β-Sheet Diffraction Peaks							
DMPG + Aβ_m	1.329*	0.071 ± 0.017	4.73 ± 0.02	-	69 ± 12	79 ± 11	35.8
DMPG + FO	1.329 ± 0.010	0.083 ± 0.012	4.73 ± 0.04	-	130 ± 13	67 ± 17	37.0
DMPG + NFO	-	-	-	-	-	-	-

*This value was fixed to reduce the number of parameters in fitting.
**Calculated as the distance between acyl tails assuming hexagonal packing

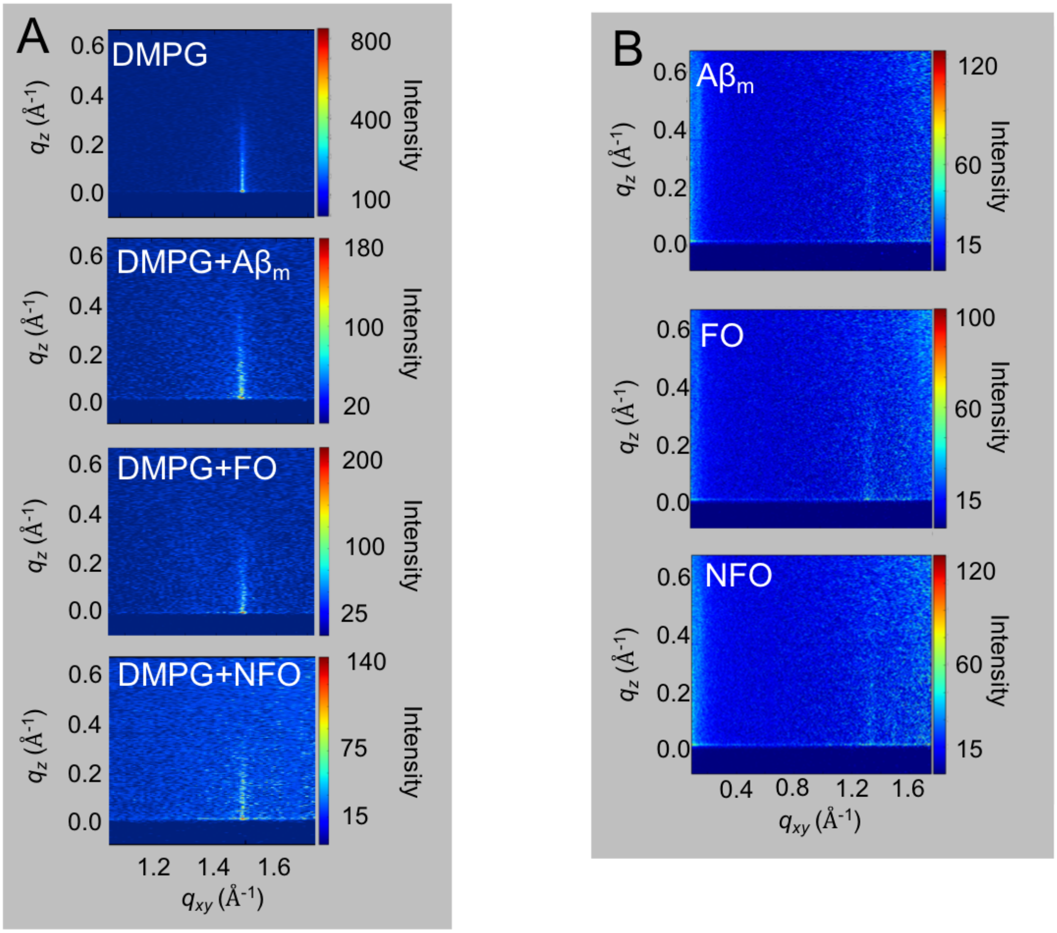

Figure S1: Two-dimensional intensity, $I(q_{xy}, q_z)$, GIXD images of diffraction peaks for (A) DMPG before and after addition of $A\beta_m$, FO, and NFO, and (B) $A\beta_m$, FO, and NFO adsorbed to an air/water interface.

References

1. Jensen, T. R., and Kjaer, K. (2001) Structural properties and interactions of thin films at the air-liquid interface explored by synchrotron x-ray scattering. *Nov. methods to study interfacial layers*
2. Als-Nielsen, J., and Kjaier, K. (1989) X-ray reflectivity and diffraction studies of liquid surfaces and surfactant monolayers. *Phase Transitions Soft Condens. Matter*
3. Als-nielsen, J., Jacquemain, D., Kj, K., Leveiller, F., Lahav, M., and Leiserowitz, L. (1994) Principles and applications of grazing incidence X-ray and neutron scattering from ordered molecular monolayers at the air-water interface. *Phys. Rep.* **246**, 251–313
4. Chi, E. Y., Ege, C., Winans, A., Majewski, J., Wu, G., Kjaer, K., and Lee, K. Y. C. (2008) Lipid membrane templates the ordering and induces the fibrillogenesis of Alzheimer's disease amyloid-β peptide. *Proteins Struct. Funct. Bioinforma.* **72**, 1–24
5. Nelson, A. (2006) Co-refinement of multiple-contrast neutron/X-ray reflectivity data using MOTOFIT. *J. Appl. Cryst.* **39**, 273–276
6. Guinier, A. (1963) *X-ray diffraction in crystals, imperfect crystals, and amorphous bodies* (Freeman, W. H. ed), San Francisco